



Enstrophy change of the Reynolds-Orr solution in channel flowPéter Tamás Nagy **Department of Hydrodynamic Systems, Faculty of Mechanical Engineering, Budapest University of Technology and Economics, Budapest H-1111, Hungary* (Received 12 July 2021; revised 30 November 2021; accepted 24 February 2022; published 21 March 2022)

The plane Poiseuille flow is one of the elementary flow configurations. Although its laminar-turbulent transition mechanism has been investigated intensively in the last century, the significant difference in the critical Reynolds number between the experiments and the theory lacks a clear explanation. In this paper, an attempt is made to reduce this gap by analyzing the solution of the Reynolds-Orr equation. Recent published results have shown that the usage of enstrophy (the volume integral of the squared vorticity) instead of the kinetic energy as the norm of perturbations predicts higher Reynolds numbers in the two-dimensional case. In addition, other research show has shown an improvement of the original Reynolds-Orr energy equation using the weighted norm in a tilted coordinate system. In this paper the enstrophy is used in three dimensions combined with the tilted coordinate system approach. The zero-enstrophy-growth constraint is applied to the classical Reynolds-Orr equation, and then the solution is further refined in the tilted coordinate system. The results are compared to direct numerical simulations published previously.

DOI: [10.1103/PhysRevE.105.035108](https://doi.org/10.1103/PhysRevE.105.035108)**I. INTRODUCTION**

The delay of the laminar-turbulent transition in the boundary layer is a promising way to achieve significant drag reduction in streamlined bodies. The transition mechanism has multiple scenarios depending on the circumstances. In the case of a high free-stream turbulence level, a proper bypass transition prediction method still does not exist. Furthermore, Fransson and Shahinfar [1] pointed out that the relevant properties of the upstream flow are not clear.

The Reynolds-Orr equation (RO) [2,3], known as the energy method, is a candidate for handling this problem. The perturbation velocity field is varied to minimize the Reynolds number such that the change of the kinetic energy is zero. If the Reynolds number is below the critical, minimal one, the kinetic energy of any perturbation cannot increase and must decay exponentially. It can be shown that this value is independent of the perturbation amplitude in the case of periodic or wall-bounded domains. Consequently, it defines the unconditional stability limit that can be determined by the solution of the variational problem [3]. This means the flow must be stable independently of the upstream flow conditions. Unfortunately, the predicted values are overly conservative and significantly below the experimental values in most cases. The explanation is that above the critical Reynolds number, certain perturbations can grow for a short time, but they decay later, which does not necessarily lead to flow oscillations or turbulence.

In our previous paper [4], an active coating on the boundary layer flow was investigated by the RO equation and the asymptotic solutions of the Orr-Sommerfeld equation (OS)

with the aim of drag reduction. The coating consists of miniature elements that move the wall in the streamwise direction proportionally to the additional shear stress of the disturbances. The eigenvalues of the Orr-Sommerfeld equation predict the linear stability limit. The results show a considerable difference in the critical Reynolds number, and the two methods predict different tendencies. According to the asymptotic stability analysis using the OS equation, the flow is stabilized with the increasing proportional controller parameter, while the RO equation predicts smaller values of the critical Reynolds number. According to the OS equation, the critical Reynolds number can significantly increase with the right choice of the parameter. On the other hand, the RO equation predicts that any streamwise movement of the wall proportional to the wall shear stress slightly destabilizes the flow. The opposite trend suggests that the coating works at low-turbulence levels, but it accelerates transition at high free-stream turbulence levels. However, the predicted critical Reynolds numbers in the latter case are impractical. The difference between the two methods is associated with the nonnormality (nonorthogonal eigenvectors) of the linear problem [2] and the transient growth of disturbances discussed by Schmid and Henningson [5]. Further research is necessary for achieving a more reliable estimation of the transition at high-turbulence levels. An improved relatively, yet relatively simple prediction method is desired for developing passive techniques to delay the laminar-turbulent transition and reduce the aerodynamic drag.

Recent studies have shown possible ways to improve the energy method or find another Lyapunov function to predict the unconditional stability limit of the flows [6–8]. These methods try to predict the nonlinear stability limit without prescribing the monotonic decay of the perturbations kinetic energy. These are possible ways to get practically more

*pnagy@hds.bme.hu

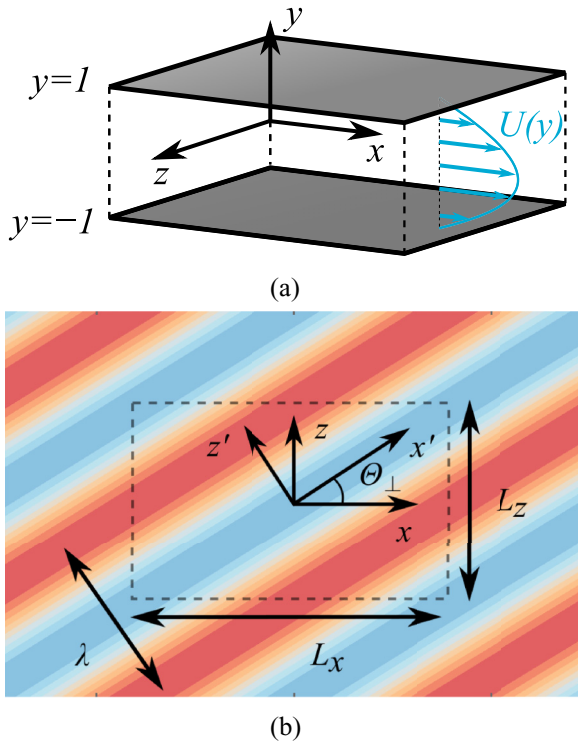


FIG. 1. (a) Schematic drawing of the domain and the base flow. (b) Schematic drawing of the perturbation in the original (x, y, z) and the tilted (x', y, z') coordinate system. The wall-normal direction (y) is unchanged. The wave number of the perturbation points into z' .

relevant critical Reynolds numbers. Falsaperla *et al.* [6] investigated the kinetic energy of disturbances in a tilted coordinate system in the case of the plane Poiseuille [Fig. 1(a)] and Couette flows. They used the weighted norm of the perturbation energy, and they found a significantly larger Reynolds number depending on the angle between the perturbation wave-number vector and the streamwise direction. Further details of their result and their formula and its criticism are shown in the Appendix. Additionally, Falsaperla *et al.* [6] found good agreement with numerical and experimental results from the literature for given wavelengths and angles in Couette and Poiseuille flows. Besides, the estimated critical Reynolds number increases in both flows roughly by a factor of 2 since the streamwise disturbances, originally assumed to be more unstable, are more stable according to the presented theory. However, the result is still conservative compared to experiments. Furthermore, their study cannot explain why the unstable solution at the lowest Reynolds numbers calculated by means of numerical simulations [9] or experiments [10] is not mainly composed of streamwise oscillating (spanwise) perturbations. Since then, the authors have used a similar theorem to investigate the Bingham-Poiseuille flow [11], magnetohydrodynamic flows [12], and open channel flow [13].

Another interesting outcome was found regarding the critical Reynolds number when the temporal change of the enstrophy was investigated instead of the weighted norm of the kinetic energy. The enstrophy is the integral of the squared disturbance vorticity over the whole domain. Fraternali *et al.*

[7] used this quantity in their study based on the original paper of Synge [14]. The derivation is similar to the Reynolds-Orr equation, but the variational method is applied to the temporal enstrophy change to minimize the Reynolds number. Below the minimal (critical) one, the enstrophy of the disturbances must decay, meaning that the kinetic energy must decay after a certain time. Unfortunately, as pointed out by the authors, in three dimensions the temporal growth of the enstrophy, contrary to that of the kinetic energy, is not independent of the amplitude. Furthermore, the variational problem is not linear but contains a quadratic term. In the derived form, their theory can be used in two dimensions only for spanwise (streamwise oscillating) perturbations where the problematic term is zero. However, the method predicts a Reynolds number ($Re_{\Omega} = 155$) significantly higher than that of the RO equation ($Re = 87.6$). The explanation for the difference can be interpreted as follows. Between the two Reynolds numbers, there are certain disturbance waves whose kinetic energy grows for a short time and decays later, while their enstrophy decays monotonically. Examples were shown to illustrate this in the cited paper. The explanation is similar to the result of Falsaperla *et al.* [6]. There, the classical norm of the disturbance velocities can increase in a certain coordinate system for a short time, but the weighted velocity norm of the disturbance wave decays below the critical Reynolds number calculated using Eq. (A1) in a tilted coordinate system. The enstrophy-based stability analysis was used for investigating channel flows with blowing and suction at the walls by Lee and Wang [8]. There are other alternative opportunities to define the generalized energy or Lyapunov function. Galdi and Padula [15] wrote a comprehensive description. Such a function was used in the investigation of Couette flow by Kaiser *et al.* [16]. They found a significantly larger Reynolds number, but surprisingly, the value was equal to the original value of Orr [2], who solved the two-dimensional problem.

An alternative way to obtain the critical Reynolds number where the flow can become turbulent is the application of numerical simulations. Although these approaches probably do not give a rigorous stability limit contrary to the methods mentioned above, they can reveal aspects of the development of periodic orbits of perturbations and turbulence. Many studies have been concerned with this topic, and therefore, giving a complete overview of the literature is beyond the scope of this study.

One breakthrough was the technique developed by Toh and Itano [17]. With their method, the unstable boundary between the stable (laminar) and the unstable (turbulent) state can be calculated in a numerically efficient way. The method calculates the amplitude of the three-dimensional perturbation by the shooting method, such that the kinetic energy remains between predefined limits during one time step. They found a periodiclike solution in the plane channel flow at the Reynolds number of 3000. Their method was used later by Zammert and Eckhardt [18]. First, they investigated and found streamwise localized perturbations at the Reynolds number of 1400. They were able to track the solution until the Reynolds number of 1038. Furthermore, they found a spanwise localized solution that was used as an initial guess on a domain extended in the spanwise direction. This initialization led to a streamwise and spanwise double-localized solution. At the same time,

reducing the Reynolds number in the direct numerical simulations (DNS) or in the experiments of a turbulent channel flow revealed oblique stripe patterns between the laminar and the fully turbulent state [10,19–21]. The long-term computation of these fields needs a large domain in both the streamwise and the spanwise directions, which is computationally very expensive. The usage of the tilted computational domain was suggested for capturing these low-Reynolds-number turbulent-laminar patterns in the case of plane Couette flow by Barkley and Tuckerman [22]. The same technique was applied on plane Poiseuille by Tuckerman *et al.* [23]. They set the tilt angle to 24° and varied the Reynolds number between 700 and 2300. They could track a single turbulent band at the lowest Reynolds number of 800. Recently, Paranjape *et al.* [9] used the same tilted domain to reduce the computational needs and carried out a thorough investigation to determine the critical Reynolds number where a traveling wave perturbation can exist for a long time. In their case, the perturbation fields were localized similarly to the investigation of Zammert and Eckhardt [18], but they were localized in the tilted z' directions. This property was verified by varying the $L_{z'}$ length. Above a certain value, the magnitude of the perturbation decays close to zero at the boundaries in the z' direction. The further increment of the $L_{z'}$ length did not effect the results. They investigated the tilt angle (Θ) and the streamwise length ($L_{x'}$) of the domain. For a fixed-length, $L_{x'} = 3.33$, the minimum Reynolds number, where the perturbation energy does not decay for a long time, was found to be 370.55 at $\Theta_{\parallel} = 45^\circ$. Here, the subscript of Θ indicates that in their coordinate system, the perturbation oscillates mainly in the x' direction. This notation expresses the angle between the wave-number vector and the original x direction here in the case of a single-wave perturbation. In the DNS simulation, the disturbance still depends on the z' variable, but it decays in that direction. At the same time, Falsaperla *et al.* [6] used the tilt angle (Θ_{\perp}) differently. The perturbation does not change in the x' direction at all and spatially oscillates along z' . The difference between the two angles is trivial, $\pi/2$. Due to the symmetry of the problem around the x axis, both angles can be defined in the range $[0, \pi/2]$ without the loss of generality. In this case, they are complementary angles.

Next, Paranjape *et al.* [9] investigated the length of the domain at the fixed tilt angle $\Theta_{\parallel} = 45^\circ$, and the new minimum Reynolds number was found to be 367 at $L_{x'} = 3.2$. However, they could not exclude the existence of a local minimum corresponding to unreported families of traveling wave solutions. However, these solutions were found at a much lower Reynolds numbers than in the case of the previously reported results. Formerly, Wall and Nagata [24] found traveling wave solutions at the Reynolds number of 665.4 at the streamwise and the spanwise wave number of 1.32 and 2.89, respectively. Later, Tao *et al.* [25] found self-sustained bands at $Re > 660$ by means of full-domain DNS initializing the problem with a turbulent band found at $Re = 900$. Another approach was used recently by Parente *et al.* [26], who minimized the energy necessary for initiating turbulence at $Re = 1000$. They solved the linear and the nonlinear optimal growth problem. In the linear case, the optimal perturbation was found at the spanwise and streamwise wave numbers of 1.2 and -1.75 , meaning that the angle of the critical initial

perturbation is $\Theta_{\parallel} = 34.5^\circ$. The critical perturbation of the nonlinear problem has a similar tilt angle, but the structure is more complex than that of a single wave. Furthermore, the solution is localized contrary to the solution of the linear problem. As the authors concluded, orders of magnitude smaller localized perturbation can trigger the turbulent state. This was verified by artificially localizing the solution of the linear problem.

Although these numerical computations can reveal many aspects of the laminar-turbulent transition, they have two significant drawbacks. First, they are computationally very expensive. Second, it is a challenging or impossible task to prove that the solution is the one at the lowest Reynolds number that does not decay to the laminar state. A further improvement of the energy method is inevitable in order to find the edge state solution. Furthermore, a simpler transition prediction method is desired for an engineering practice that can be used for the investigation of various control techniques.

In this paper, the effect of the zero-entropy-growth constraint on the classical RO equation is investigated in the channel flow. The hypothesis is that the edge state disturbance is close to the disturbances whose kinetic energy and entropy do not grow or decay. First, the derivation of the equation and the solution method are introduced in Sec. II. Then, the equation is solved as a modal problem, and the entropy change is evaluated for various wave numbers. Next, the results are shown in Sec. III. After that, the critical Reynolds number is improved using the formula of Falsaperla *et al.* [6]. The results are compared to the numerical investigation of Paranjape *et al.* [9]. Finally, concluding remarks are made in Sec. IV.

II. THEORY AND SOLUTION METHOD

The evolution of a perturbed flow field can be described by the following nondimensional form of the Navier-Stokes equations:

$$\frac{\partial u_i}{\partial t} = -U_j \frac{\partial u_i}{\partial x_j} - u_j \frac{\partial U_i}{\partial x_j} - u_j \frac{\partial u_i}{\partial x_j} - \frac{\partial p}{\partial x_i} + \frac{1}{Re} \frac{\partial^2 u_i}{\partial x_j^2} \quad (1)$$

and the continuity equation

$$\frac{\partial u_i}{\partial x_i} = 0. \quad (2)$$

U_i is the base flow velocity, u_i is the perturbation velocity, and p is the pressure. Re is the Reynolds number defined as

$$Re = \frac{U_0 h}{\nu}, \quad (3)$$

where U_0 is the maximum velocity at the center line, h is the half gap, and ν is the kinematic viscosity. The domain is a cuboid, $x = x_1 \in [0, L_x]$, $y = x_2 \in [-1, 1]$, and $z = x_3 \in [0, L_z]$, which can be seen in Fig. 1(a). The domain is periodic in the streamwise, x , and spanwise, z , directions. At $y = \pm 1$, no-slip wall boundary conditions hold. The base flow is the well-known parabolic profile

$$U_i = U(x_2)\delta_{i1} = (1 - x_2^2)\delta_{i1}, \quad (4)$$

where δ_{ij} is the Kronecker delta. The perturbation kinetic energy is

$$e = \frac{1}{2} \int_{\mathcal{V}} u_i^2 d\mathcal{V}. \quad (5)$$

Its temporal change can be calculated by multiplying Eq. (1) by u_i and integrating it over the whole domain. Using the Gauss divergence theorem, some terms are eliminated or rewritten, knowing that the velocity and the pressure perturbations are periodic in the x and z directions, and the velocity is zero at the walls. After simplification, the expression is

$$\frac{de}{dt} = \int_{\mathcal{V}} \left(-u_i u_j \frac{\partial U_i}{\partial x_j} - \frac{1}{\text{Re}} \frac{\partial u_i}{\partial x_j} \frac{\partial u_i}{\partial x_j} \right) d\mathcal{V}. \quad (6)$$

The first term on the right-hand side is identified as the production and the second one is the dissipation of the kinetic energy. Minimizing the Reynolds number, where the temporal change of the kinetic energy is zero, leads to a variational problem. The i th component of the corresponding Euler-Lagrange equation of Eq. (6) is

$$-u_j \left(\frac{\partial U_i}{\partial x_j} + \frac{\partial U_j}{\partial x_i} \right) + \frac{2}{\text{Re}} \frac{\partial^2 u_i}{\partial x_j^2} - \frac{\partial q}{\partial x_i} = 0, \quad (7)$$

where the Lagrange multiplier q was added to the functional to prescribe divergence-free perturbations. This is the RO equation. Equations (7) and (2) form an eigenvalue problem for the Reynolds number, and the smallest real solution is the valid one.

The enstrophy (s) is the volume integral of the squared disturbance vorticity (ω_i):

$$\omega_i = -\epsilon_{ijk} \frac{\partial u_j}{\partial x_k}, \quad (8)$$

$$s = \frac{1}{2} \int_{\mathcal{V}} \omega_i^2 d\mathcal{V}, \quad (9)$$

where ϵ_{ijk} is the Levi-Civita symbol. The temporal evolution of the disturbance enstrophy can be calculated as

$$\begin{aligned} \frac{ds}{dt} = \int_{\mathcal{V}} \left(-\omega_i u_j \frac{\partial \Omega_i}{\partial x_j} + \omega_i \Omega_j \frac{\partial u_i}{\partial x_j} \right. \\ \left. + \omega_i \omega_j \frac{\partial u_i}{\partial x_j} + \omega_i \omega_j \frac{\partial U_i}{\partial x_j} + \frac{1}{\text{Re}} \omega_i \frac{\partial^2 \omega_i}{\partial x_j^2} \right) d\mathcal{V}, \quad (10) \end{aligned}$$

where Ω_i is the base flow vorticity. In this case, the last integrand

$$\int_{\mathcal{V}} \frac{1}{\text{Re}} \omega_i \frac{\partial^2 \omega_i}{\partial x_j^2} d\mathcal{V} \neq \int_{\mathcal{V}} -\frac{1}{\text{Re}} \frac{\partial \omega_i}{\partial x_j} \frac{\partial \omega_i}{\partial x_j} d\mathcal{V}, \quad (11)$$

and since the vorticity is nonzero on the walls, the term cannot be simplified using the Gauss divergence theorem. The presence of the third integrand in Eq. (10) causes the temporal growth rate of the enstrophy, $\frac{1}{s} \frac{ds}{dt}$, to depend on the amplitude of the perturbation contrary to the growth rate of the kinetic energy. The third term scales with the amplitude to the power of 3, while the enstrophy and the other terms scale to the power of 2. However, the third term is zero for a single periodically oscillating mode. It can be only nonzero on the periodic domain if multiple modes are present. From this point

on, the investigation is restricted to single-wave perturbations. This assumption reduces the universality of the outcome of the paper, but the results are more general than assuming two-dimensional perturbations that were investigated recently by Fraternali *et al.* [7]. Furthermore, if the perturbation is small, the problematic term is 1 order of magnitude smaller than the others. The constraint is applied in the following way. The original RO equation is solved for the Reynolds number on a modal basis at various streamwise and spanwise wave-number pairs (α, β) , and then the enstrophy change is evaluated for each mode. Since the solution of RO fulfills the zero-energy-change condition, the wave-number pairs are selected where the enstrophy change is zero. The critical Reynolds number is the smallest one among these solutions. Since the enstrophy change constraint can be fulfilled with the sum of other modes, the predicted critical Reynolds number is not a mathematically strict limit like that derived from the original method or the results of Falsaperla *et al.* [6]. However, a physically reasonable assumption is that the most critical perturbation is a single wave, according to the energy theory. Here, this theory is supplemented by the enstrophy constraint. This analysis can reveal the long-living, critical traveling wave solution in the flow.

The modal solution has the following form:

$$u_i = \hat{u}_i(y) \exp [i(\alpha x + \beta z)], \quad (12)$$

$$q = \hat{q}(y) \exp [i(\alpha x + \beta z)], \quad (13)$$

where $\alpha = 2\pi/L_x$ and $\beta = 2\pi/L_z$. The wavelength of the perturbation can be calculated as $\lambda = 2\pi/\sqrt{\alpha^2 + \beta^2}$. The general eigenvalue problem for the eigenvalue (Re) and the eigenfunctions $[\hat{u}_i(y), \hat{q}_m(y)]$ can be summarized from Eqs. (2) and (7) in a matrix form as

$$\begin{bmatrix} 2L & 0 & 0 & -i\alpha \\ 0 & 2L & 0 & -D \\ 0 & 0 & 2L & -i\beta \\ i\alpha & D & i\beta & 0 \end{bmatrix} \begin{bmatrix} \hat{u}_1 \\ \hat{u}_2 \\ \hat{u}_3 \\ \hat{q}_m \end{bmatrix} = \text{Re} \begin{bmatrix} 0 & \frac{dU}{dy} & 0 & 0 \\ \frac{dU}{dy} & 0 & 0 & 0 \\ 0 & 0 & 0 & 0 \\ 0 & 0 & 0 & 0 \end{bmatrix} \begin{bmatrix} \hat{u}_1 \\ \hat{u}_2 \\ \hat{u}_3 \\ \hat{q}_m \end{bmatrix}, \quad (14)$$

after substituting Eqs. (12) and (13) into Eqs. (2) and (7). $L = D^2 - (\alpha^2 + \beta^2)$ is the Laplace operator and $D = \frac{d}{dy}$ is the differential operator. The introduction of $\hat{q}_m = \hat{q}/\text{Re}$ is advantageous since then the numerically discretized operator on the left-hand side is not singular. This reduces the number of the spurious modes appearing in the numerical calculation. The problem is discretized by means of the Chebyshev collocation method with $N = 60$ polynomials, similarly to the investigation of Falsaperla *et al.* [6]. The wall boundary condition $\hat{u}_i(y = \pm 1) = 0$ is prescribed for each velocity component. The method is implemented in MATLAB 2019b, and the eigenvalue problem is solved using the built-in function eig.

The code is verified by data from the literature. The minimal Reynolds number is determined for the most critical spanwise and streamwise perturbation. The spanwise problem is solved using series expansion by MacCreadie [27]. His min-

imum is $Re = 87.63$ using the notation of this paper, but he defined the Reynolds number based on the gap width and the mean velocity of the base flow. The minimal Reynolds number found using the presented technique is $Re = 87.593\,68$ at $\alpha = 2.098\,599$. The critical Reynolds number in the case of a streamwise perturbation is $Re = 49.6035$ at $\beta = 2.044$ according to Busse [28]. (The values are converted since he defined the Reynolds number based on the gap width.) The minimal Reynolds number is $Re = 49.603\,578$ at $\beta = 2.043\,697$ using the presented technique. The values are in good agreement with data published previously in both cases.

III. RESULTS AND DISCUSSION

The problem is solved on a fine grid of wave numbers. α is varied between 0.02 and 8 with the resolution of $\Delta\alpha = 0.05$ and $\beta \in [0, 8]$ with the resolution of $\Delta\beta = 0.05$. The critical Reynolds numbers as a function of wave numbers are plotted in Fig. 2(a). As well known from the literature [29], the most critical perturbations belong to spanwise oscillating cases. However, for a large range of parameters it does not change significantly. For example, the change of the critical Reynolds number is less than 10% larger than the most critical value in the domain of $\alpha \in [0, 0.75]$ and $\beta \in [1.5, 2.75]$.

The temporal growth rate of the enstrophy,

$$\mu_s = \frac{1}{s} \frac{ds}{dt}, \quad (15)$$

is evaluated using Eqs. (9) and (10). See Supplemental Material [30] for growth rate values and the critical Reynolds number in the MATLAB data format. The growth rate is plotted in Fig. 2(b). In the case of spanwise perturbations ($\alpha \neq 0$, $\beta = 0$) at the bottom of the figure, the enstrophy decreases. This is the expected result since the calculated Reynolds number is much smaller than the enstrophy-based one (155) [7]. Below the critical Reynolds number for the enstrophy change, the enstrophy must decay. However, as the tilt angle of the perturbation wave is increased, the temporal enstrophy change increases. It changes sign at $\Theta_{\parallel} = 45^\circ$ for long waves and at higher angles for shorter waves. Furthermore, the critical Reynolds number decreases as the wave-number vector rotates toward the spanwise direction. This means that the enstrophy can grow for tilted perturbations easily, and the enstrophy-based critical Reynolds number must be lower than the energy-based one for streamwise perturbations ($\alpha = 0$, $\beta \neq 0$). The further consequence of this result is that the enstrophy-based stability analysis would predict a critical Reynolds number, in a three-dimensional case, lower than the kinetic energy-based one. It must be mentioned that the result of Fraternali *et al.* [7] was valid only in two dimensions for spanwise perturbations and their enstrophy-based analysis predicts a much higher critical Reynolds number only in that case. The usage of an enstrophy-based stability analysis is not beneficial on its own in three-dimensional flows, even if the problematic term is neglected.

However, these results do not explain why streamwise ($\alpha = 0$, $\beta \neq 0$) perturbations are not the most critical ones. Both enstrophy-based and classical kinetic energy-based analyses would predict that. According to the energy theory, the critical Reynolds number is smaller in that case, and the

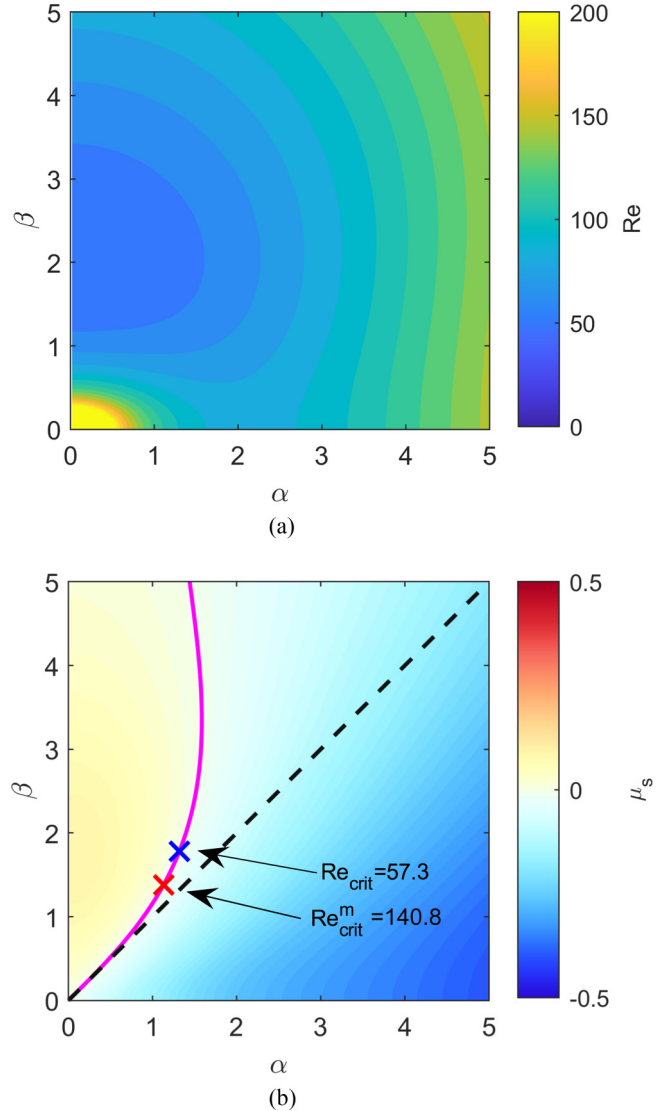


FIG. 2. (a) The Reynolds number (original RO equation) and (b) the temporal growth rate of the enstrophy as a function of the streamwise (α) and spanwise (β) wave numbers for the most critical perturbation according to the RO equation. The solid magenta line represents the zero growth of enstrophy. The black dashed line shows the perturbations where the angle between the wave-number vector and the streamwise direction is 45° . The most critical perturbation with zero enstrophy growth was found at $\alpha = 1.32$, $\beta = 1.78$, and $Re_{\text{crit}} = 57.3$ according to the original RO equation and at $\alpha = 1.13$, $\beta = 1.38$, and $Re_{\text{crit}}^m = 140.8$ according to the method of Falsaperla *et al.* [6].

enstrophy increases, too. The explanation can be given following the theory of Falsaperla *et al.* [6], who introduced a weighted norm for the kinetic energy. They showed that the critical Reynolds number with the new norm must increase as the angle of perturbation (Θ_{\parallel}) increases. According to their theory, a spanwise perturbation should be the critical one, but the enstrophy-based analysis suggests that a streamwise perturbation is the most critical one. Furthermore, enstrophy-based analysis predicts a Reynolds number higher than that of the theory of Falsaperla *et al.* [6] in the case of spanwise

perturbations. The contradiction of the two results implies that the critical perturbation should be a tilted one between the streamwise and spanwise directions. This is a possible explanation for the phenomena observed in experiments [10] and numerical simulations [9,19–21].

In Fig. 2(b), a single, continuous line shows the wave-number components where both the enstrophy and kinetic energy neither grow nor decay initially. For small wave numbers ($\alpha, \beta < 1$) and large wavelengths ($\lambda > 5$), the critical perturbation oscillates in the direction with an angle of 45° to the streamwise direction (black dashed curve in the figure). This finding agrees well with the literature. The systematic optimization procedure of Paranjape *et al.* [9] found the most critical traveling wave solution on the domain tilted with an angle of 45° . Attempts are made to explain this observation. First, the terms of the enstrophy change (10) are analyzed. It can be shown that the first term

$$\int_{\mathcal{V}} \left(-\omega_i u_j \frac{\partial \Omega_i}{\partial x_j} \right) = \int_{\mathcal{V}} \left(\frac{\partial \omega_i}{\partial x_j} u_j \Omega_i \right) d\mathcal{V} \quad (16)$$

since

$$\int_{\mathcal{V}} \frac{\partial}{\partial x_j} (\omega_i u_j \Omega_i) = 0 \quad (17)$$

according to the Gauss divergence theorem. Using Eq. (16), it can be derived that the integral of the first term in Eq. (10) is equal to the second term in the case of a single-wave perturbation and parallel base flow:

$$\begin{aligned} \int_{\mathcal{V}} \left(-\omega_i u_j \frac{\partial \Omega_i}{\partial x_j} \right) &= \int_{\mathcal{V}} \left(\omega_i \Omega_j \frac{\partial u_i}{\partial x_j} \right) d\mathcal{V} \\ &= L_x L_z \int_{-1}^1 \left[R \left(\hat{u}_2, \frac{d^2 \hat{u}_1}{dx_2^2} \right) \right. \\ &\quad \left. + R \left(i \frac{d\hat{u}_2}{dx_2}, i \frac{d\hat{u}_1}{dx_2} \right) \right] \Omega_3 dx_2, \quad (18) \end{aligned}$$

where $R(a, b) = \Re(a)\Re(b) + \Im(a)\Im(b)$. $\Re()$ and $\Im()$ are the real and imaginary parts of a complex number, respectively. Relation (18) is striking and surprisingly simple. The third term in Eq. (10) is zero in the case of a single perturbation wave, as it was discussed in Sec. II. Unfortunately, the remaining two terms cannot be significantly simplified. All of the nonzero terms in the integrand were plotted in Fig 3. The results showed that the first and second terms are positive in the case of critical perturbations [Fig 3(a)]. They have a maximum roughly at $\alpha = 0$ and $\beta = 1.75$ that is close to the location of the most critical perturbation according to energy theory ($\alpha = 0, \beta = 2.04$). Far from this point, their effect becomes insignificant. These two terms dominate the enstrophy production for long waves and cause the enstrophy change of the critical perturbations with 45° tilt angle to be zero. The fourth term [Fig. 3(b)] is negative in the case of very long perturbation waves (small α and β values), increases rapidly with the spanwise wave number, and dominates the overall enstrophy production as $\beta > 2$. The fifth term expresses the dissipation [Fig. 3(c)], and its value is always negative. As the wavelength of the perturbation is reduced (increasing α and β), the absolute value increases significantly, as expected, because of the effect of the Laplacian operator. In the case

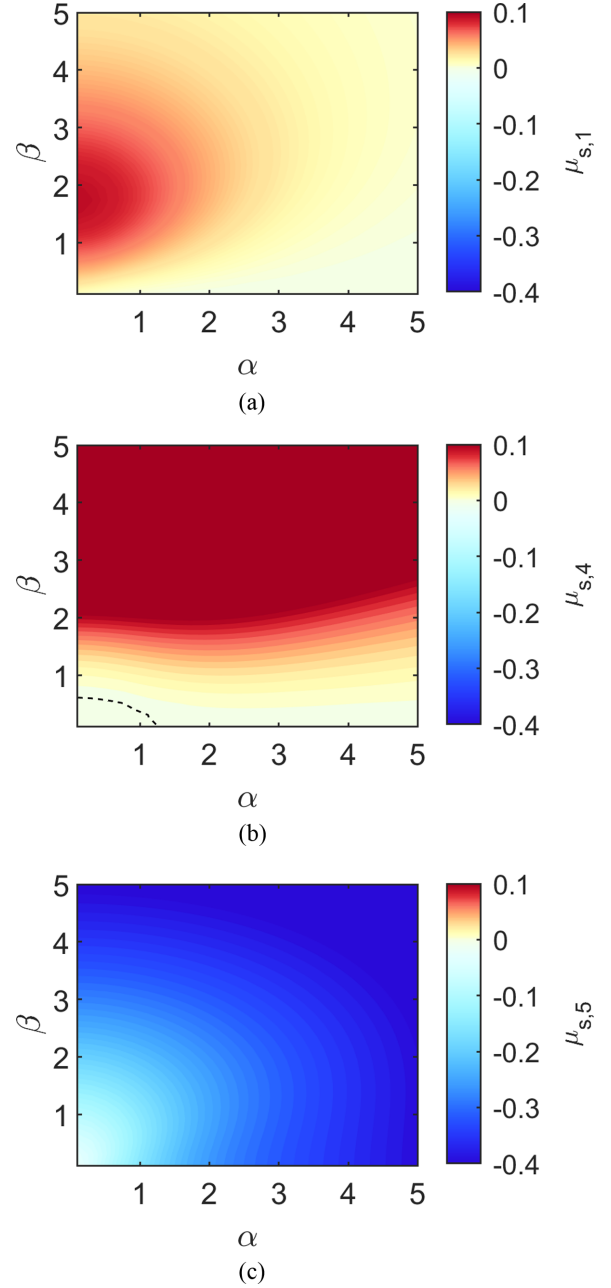


FIG. 3. The terms of the enstrophy change in the integrand of Eq. (10) normalized by the enstrophy in the case of the critical perturbations according to the Reynolds-Orr energy theory. (a) First and second terms: $1/s \int_{\mathcal{V}} -\omega_i u_j \frac{\partial \Omega_i}{\partial x_j} d\mathcal{V} = 1/s \int_{\mathcal{V}} \omega_i \Omega_j \frac{\partial u_i}{\partial x_j} d\mathcal{V}$. (b) Fourth term: $1/s \int_{\mathcal{V}} \omega_i \omega_j \frac{\partial u_i}{\partial x_j} d\mathcal{V}$. (c) Fifth term: $1/s \int_{\mathcal{V}} \frac{1}{\text{Re}} \omega_i \frac{\partial^2 \omega_i}{\partial x_j^2} d\mathcal{V}$. In panel (b), the dashed line represents the zero enstrophy growth.

of short waves, the overall enstrophy change is dominated by the fourth and fifth terms. Since the production of the fourth term increases mainly with the spanwise wave number β , and the dissipation (the opposite of the fifth term) increases with the wave number $\sqrt{\alpha^2 + \beta^2}$, the perturbations with zero change of enstrophy have a larger spanwise wave number than a streamwise one. This explains why the tilt angle of the

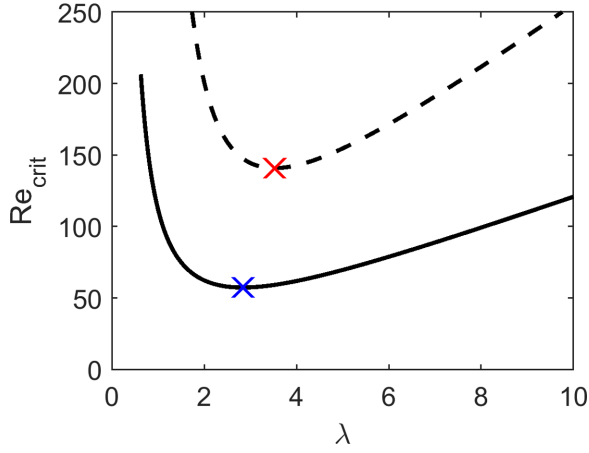


FIG. 4. The critical Reynolds number as a function of the wavelength in the case of perturbations with zero change of enstrophy. The continuous line is the classical solution and the dashed line is the improved solution, according to Eq. (A1). The two crosses represent the minima.

short critical perturbation waves with zero enstrophy change is larger than 45° . However, the physical mechanism behind the observations remains unrevealed.

In the next step, a heuristic search for the most critical perturbation is carried out. It is assumed that, in the case of the critical perturbation, both the kinetic energy and the enstrophy should be in a neutrally stable state. The wave-number pairs of such kind of perturbations belong to the continuous line in Fig. 2(b). The zero enstrophy growth curve can be expressed as a function of β . In this step, β is varied between 0.02 and 10 with the resolution of $\Delta\beta = 0.02$. The corresponding α value, where the enstrophy growth is zero, is determined utilizing the built-in function *fminsearch*. The initial guess comes from the previous results. For that wave number and tilt angle, the critical Reynolds number is obtained, and a further estimation is carried out making use of the corrected formula (A2) of Falsaperla *et al.* [6]. The wavelength and the tilt angle were determined from the wave-number pairs. Since Falsaperla *et al.* [6] assumed that the perturbations vary along the z' axis, the tilt angle can be calculated as

$$\Theta_{\perp} = \left| \arctan \left(\frac{\alpha}{\beta} \right) \right|. \quad (19)$$

The absolute value is calculated since the results are invariant to the sign of the wave numbers, and Θ_{\perp} is defined here between 0 and $\pi/2$.

The critical Reynolds number calculated using the classical equation and the modified theory are plotted in Fig. 4. Among the original theory solutions, the minimum Reynolds number of zero-enstrophy-growth perturbations is 57.3 at $\alpha = 1.32$ and $\beta = 1.78$, and the wavelength is $\lambda = 2.83$. The angle between the streamwise direction and the wave-number vector is $\Theta_{\parallel} = 53.5^\circ$. The eigenfunctions (\hat{u} , \hat{v} , \hat{w}) of this most critical perturbation wave are plotted in Fig. 5, and the velocity components of the perturbation are plotted as a function of streamwise and wall-normal coordinates in Fig. 6. The velocity field is nonlocalized in this case. This is the consequence of the Reynolds-Orr equation being a linear equation de-

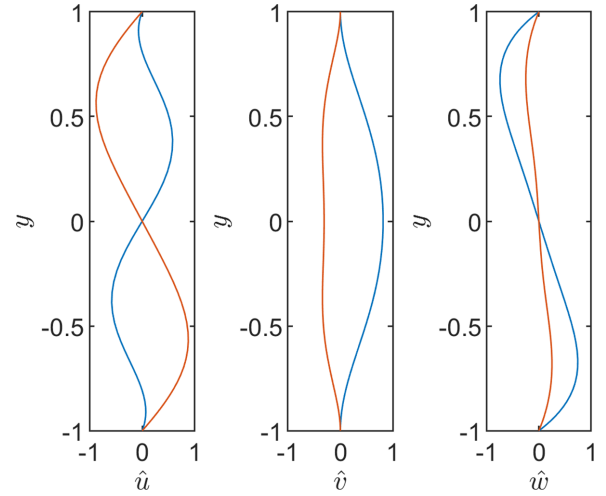


FIG. 5. The critical perturbation field according to the original theory, in which case the enstrophy change is zero. From left to right: Streamwise component, wall-normal component, and spanwise component. The blue curves are the real part and the red curves are the imaginary part of the eigenfunction.

spite describing the nonlinear stability limit. Furthermore, the components of the velocity field have the same magnitude. Although Parente *et al.* [26] optimized the perturbation field at a given Reynolds number which is notably larger, $Re = 1000$, the comparison of this result with theirs can be interesting. First, they optimized the perturbation field to obtain maximal

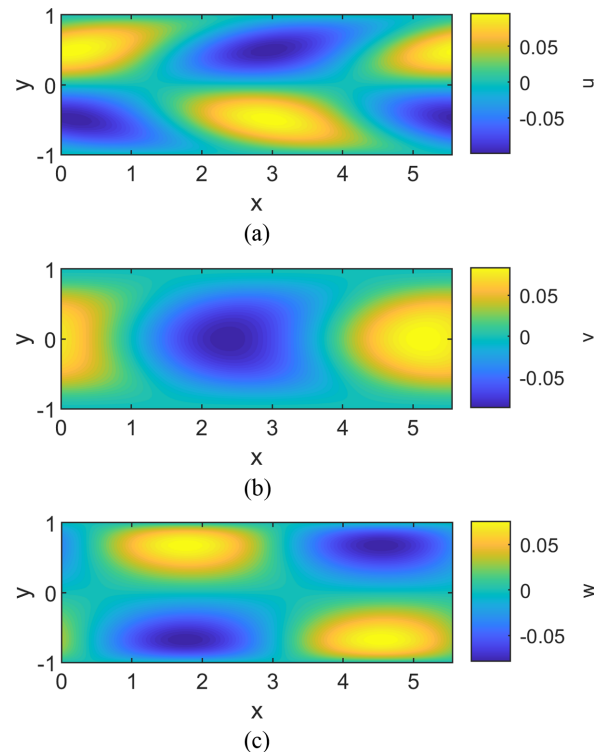


FIG. 6. The components of the critical perturbation field according to the original theory at $z = 0$ ($Re = 57.3$, $\alpha = 1.32$, $\beta = 1.78$): (a) the streamwise component, (b) the wall-normal component, and (c) the spanwise component.

growth in the linear case. They found that the optimal tilt angle of the perturbation wave is $\Theta_{\parallel} 34.5^\circ$ and their analysis predicted that the wall-normal component is larger than the others. Second, they optimized the initial perturbation field with minimal initial-energy-triggering turbulence by means of a nonlinear simulation. In this case, the magnitudes of the optimal initial-velocity field components were equal. The shape of the eigenfunctions (the amplitude of the perturbation wave as a function of the wall-normal coordinate) was completely different in both cases compared to this analysis. At the same, the aim of the two methods is significantly different.

In the next step, the modified theory of Falsaperla *et al.* [6] is applied to the problem. The most critical Reynolds number increases by a factor of 2 to 140.8 at $\alpha = 1.13$ and $\beta = 1.38$. The wavelength of the most critical perturbation is $\lambda = 3.52$. The angle between the streamwise direction and the wavenumber vector is $\Theta_{\parallel} = 50.7^\circ$. At the same time, the shape of the perturbation wave remains very similar to the velocity fields in Figs. 5 and 6 since the wave numbers are very close to that case.

The smallest Reynolds number, where a traveling wave solution on the tilted domain can exist, was found to be 367 at the tilt angle $\Theta_{\parallel} = 45^\circ$ from DNS simulations by Paranjape *et al.* [9]. Their angle of minima is very close to the result with the zero enstrophy growth and the improved theory. Furthermore, they varied the tilt angle in their study between 25° and 60° with the resolution of 5° first. Then, they fixed the tilt angle at 45° , and only the length of the domain was varied. The authors pointed out that their approach does not certainly predict the smallest critical Reynolds number. However, it is probably close to that value. The minimum Reynolds number in the numerical simulation was obtained at $L'_x = 3.2$. The most energy content is associated with the perturbation wave at a wavelength equal to the size of the domain. In my analysis, the critical wavelength is 3.52 according to the improved theory, which is only a 10% longer wavelength than that of the DNS result. The predicted critical Reynolds number (140.8) is better than the values from previous theories (49.6, 87.6), but it still underestimates the value by a factor of 2.6 compared to the DNS (367). Furthermore, it must be mentioned that the solution of the RO equation is computationally orders of magnitude less expensive than a DNS analysis. The data that support the findings of this study are available within the Supplementary Material [30].

IV. CONCLUSION

The stability of channel flow is investigated. The classical Reynolds-Orr equation is solved in a modal framework, and it is improved in two ways. First, the zero-enstrophy-growth constraint is added to the problem. The restriction narrows down the parameter space to a single curve in the wave-number plane. In the case of large wavelengths ($\alpha, \beta < 1 \rightarrow \lambda > 5$, where the length scale is the half gap), the angle between the oscillation and the streamwise direction is 45° . Next, the theory of Falsaperla *et al.* [6] is applied to these wave-number pairs. This method predicts a significantly higher Reynolds number for tilted perturbations. The critical Reynolds number is found to be 140.8 at a wavelength of 3.52 with a tilt angle of 51° . The angle and the

wavelength are in good agreement with numerical simulations from the literature. The predicted critical Reynolds number is still significantly smaller than that from the DNS simulations. At the same time, the new value is 3 times larger than the most critical one according to the classical theory (49.6) and 1.5 times larger than the one resulting from the theory of Falsaperla *et al.* [6] (87.6). This study explains by nonlinear stability analysis why the tilted waves are the critical ones.

Applying further constraints or using other norms (weighted norms, enstrophy) may provide a more accurate estimation of the critical Reynolds number and reduce the gap between theory, simulations, and experiments in the transition mechanism of the channel flow.

ACKNOWLEDGMENTS

The work has been performed within the framework of Nemzeti Kutatási Fejlesztési és Innovációs Hivatal (NKFI) Project No. K124939. I am grateful to Péter Rucz of the Budapest University of Technology and Economics for improving the text of the paper.

APPENDIX: ABOUT THE CRITICAL REYNOLDS NUMBER ESTIMATION ON TILTED DOMAINS

Falsaperla *et al.* [6] stated that the usage of the classical L_2 kinetic energy integral norm of perturbations, $e = ||u|| + ||v|| + ||w||$ is not optimal for the nonlinear stability investigation. u , v , and w are the perturbation velocity fields in the streamwise, wall-normal, and transversal directions, respectively. They used a special norm of the perturbation velocity in the tilted coordinate system, where the first velocity component has a constant multiplier (weight). They proved mathematically that the $\frac{1}{2}(C||u'|| + ||v'|| + ||w'||)$ energy will decrease for a properly chosen C parameter, if the Reynolds number is below the critical one obtained as the variation of the temporal change of $\frac{1}{2}(||v'|| + ||w'||)$. (The prime indicates the velocity fields in the tilted coordinate system.) This variational problem leads to the same equation as the classical Reynolds-Orr equation for a spanwise perturbation, if $\text{Re}_{\text{Orr}} = \text{Re} \sin \Theta_{\perp}$ is substituted and the velocity fields are properly changed. Θ_{\perp} is the tilt angle when the x' direction is perpendicular to the wave-number vector of a single-wave disturbance that can be seen in Fig. 1(b). $\bar{\text{Re}}$ is the critical Reynolds number for the weighted norm in the tilted coordinate system, while Re_{Orr} is the original solution. Here, the streamwise disturbance is defined as a wave that oscillates spatially in the spanwise direction, independent of the streamwise coordinate. Similarly, the spanwise disturbance does not change in the spanwise direction and oscillates spatially in the streamwise direction. The configuration can be seen in Fig. 1(b). x is the coordinate in the streamwise direction, y is the coordinate in the wall-normal direction, and z is the coordinate in the spanwise direction. (In the cited paper, y was the spanwise direction and z was the wall-normal direction. Their results are presented with the notation of this paper.)

Falsaperla *et al.* [6] gave the following relation between the original critical Reynolds number and the new one:

$$\bar{\text{Re}} = \frac{\text{Re}_{\text{Orr}} \left(\frac{2\pi}{\lambda \sin \Theta_{\perp}} \right)}{\sin \Theta_{\perp}}, \quad (\text{A1})$$

where λ is the wavelength of the perturbation. Below this Reynolds number, the previously defined norm of any single-wave perturbation must decay monotonically even if the classical energy norm can increase. However, the two statements imply that the classical energy can grow only for a short time and must decay later. In this case, the flow is nonlinearly stable, but it is not monotonically stable. From a practical point of view, the determination of the nonlinear limit is more important than the strict monotonically stable limit since turbulence cannot even develop in the former case.

At the same time, I argue that the division with $\sin \Theta_{\perp}$ is not necessary in the argument of the function. In Ref. [6], Eq. (A9) together with the continuity equation is the same as the classical Reynolds-Orr equation, after the substitutions mentioned previously. In the following steps, a coordinate transformation to the original system of coordinates was used, and the solution assumed the form $v(x, y) = \tilde{v}(y) \exp(iax)$. This means that the parameter a in the cited paper is the wave number in the original coordinate system, not in the tilted one. In my opinion, the critical Reynolds number of the weighted energy change for a tilted perturbation is

$$\bar{\text{Re}} = \frac{\text{Re}_{\text{Orr}}\left(\frac{2\pi}{\lambda}\right)}{\sin \Theta_{\perp}} = \frac{\text{Re}_{\text{Orr}}(\beta')}{\sin \Theta_{\perp}}, \quad (\text{A2})$$

where β' is the wave number in the z' direction.

Although the relation (A1) or (A2) is similar to the Squire theorem [31], it was obtained for the nonlinear energy equation instead of the linear Orr-Sommerfeld equation. However, the consequences of the two theorems are similar: the spanwise perturbations (oscillating in the streamwise direction) become unstable first, since the minimum of expression (A1) is at $\Theta_{\perp} = \pi/2$, meaning that the critical perturbation changes only in the $z' = -x$ direction. In this case, this equation is basically identical to the original Reynolds-Orr equation using its symmetry property. Furthermore, any streamwise (spanwise oscillating) perturbation must be stable, since $\bar{\text{Re}} \rightarrow \infty$ for $\Theta_{\perp} = 0$. This statement agrees with the result of Moffatt [32], who proved that a streamwise perturbation is always stable. Falsaperla *et al.* [6] generalized his theorem. This outcome seems to contradict the result of Joseph and Carmi [29] who found that the critical Reynolds number is 49.6 (using the Re definition of this paper) for a streamwise perturbation. The conflict can be resolved by the fact that the choice of classical norm used by Joseph and Carmi [29] is not the best one. The weighted norm of a streamwise perturbation must decay and the flow is stable; even though the classical kinetic energy of the perturbation can grow for a short time. The consequence of this is that Orr's original solution [2] is a better estimation for the nonlinear stability limit. According to the theorem of Falsaperla *et al.* [6], a spanwise perturbation is the most critical one.

-
- [1] J. H. M. Fransson and S. Shahinfar, *J. Fluid Mech.* **899**, A23 (2020).
- [2] W. M. Orr, *Proc. R. Ir. Acad.* **27**, 69 (1907).
- [3] P. Schmid and D. S. Henningson, *Stability and Transition in Shear Flows* (Springer, New York, 2001), Vol. 142.
- [4] P. T. Nagy and G. Paál, *Phys. Fluids* **31**, 124107 (2019).
- [5] P. J. Schmid, *Annu. Rev. Fluid Mech.* **39**, 129 (2007).
- [6] P. Falsaperla, A. Giacobbe, and G. Mulone, *Phys. Rev. E* **100**, 013113 (2019).
- [7] F. Fraternali, L. Domenicale, G. Staffilani, and D. Tordella, *Phys. Rev. E* **97**, 063102 (2018).
- [8] H. Lee and S. Wang, *J. Fluid Mech.* **877**, 1134 (2019).
- [9] C. S. Paranjape, Y. Duguet, and B. Hof, *J. Fluid Mech.* **897**, A7 (2020).
- [10] A. Prigent, G. Grégoire, H. Chaté, and O. Dauchot, *Phys. D (Amsterdam, Neth.)* **174**, 100 (2003).
- [11] P. Falsaperla, A. Giacobbe, and G. Mulone, *Fluids* **5**, 141(2020).
- [12] P. Falsaperla, A. Giacobbe, and G. Mulone, *Int. J. Non-Linear Mech.* **123**, 103490 (2020).
- [13] P. Falsaperla, A. Giacobbe, and G. Mulone, *Ric. Mat.* **70**, 67 (2021).
- [14] J. L. Synge, *Semcentenn. Publ. Amer. Math. Soc.* **2**, 227 (1938).
- [15] G. P. Galdi and M. Padula, *Arch. Ration. Mech. Anal.* **110**, 187 (1990).
- [16] R. Kaiser, A. Tilgner, and W. von Wahl, *SIAM J. Math. Anal.* **37**, 438 (2005).
- [17] S. Toh and T. Itano, *J. Fluid Mech.* **481**, 67 (2003).
- [18] S. Zammert and B. Eckhardt, *J. Fluid Mech.* **761**, 348 (2014).
- [19] S. Hashimoto, A. Hasobe, T. Tsukahara, Y. Kawaguchi, and H. Kawamura, in *Proceedings of the Sixth International Symposium On Turbulence Heat and Mass Transfer, 2009, 14–18 Sept., Rome, Italy* (Begell House, Danbury, CT, 2009).
- [20] K. Fukudome and O. Iida, *J. Fluid Sci. Technol.* **7**, 181 (2012).
- [21] X. Xiong, J. Tao, S. Chen, and L. Brandt, *Phys. Fluids* **27**, 041702 (2015).
- [22] D. Barkley and L. S. Tuckerman, *Phys. Rev. Lett.* **94**, 014502 (2005).
- [23] L. S. Tuckerman, T. Kreilos, H. Schrobsdorff, T. M. Schneider, and J. F. Gibson, *Phys. Fluids* **26**, 114103 (2014).
- [24] D. P. Wall and M. Nagata, *J. Fluid Mech.* **788**, 444 (2016).
- [25] J. J. Tao, B. Eckhardt, and X. M. Xiong, *Phys. Rev. Fluids* **3**, 011902(R) (2018).
- [26] E. Parente, J.-C. Robinet, P. D. Palma, and S. Cherubini, *J. Fluid Mech.* **938**, A25 (2022).
- [27] W. T. MacCreadie, *Proc. Natl. Acad. Sci. USA* **17**, 381 (1931).
- [28] F. H. Busse, *Z. Angew. Math. Phys.* **20**, 1 (1969).
- [29] D. D. Joseph and S. Carmi, *Q. Appl. Math.* **26**, 575 (1969).
- [30] See Supplemental Material at <http://link.aps.org/supplemental/10.1103/PhysRevE.105.035108> for growth rate values and the critical Reynolds number in the MATLAB data format.
- [31] H. B. Squire, *Proc. R. Soc. London, Ser. A* **142**, 621 (1933).
- [32] K. Moffatt, in *Whither Turbulence*, Lecture Notes in Physics Vol. 357, edited by J. L. Lumley (Springer-Verlag, Berlin, 1990), p. 250.